

Nonlinear Analysis on Flutter of FGM Plates Using Ilyushin Supersonic Aerodynamic Theory

Pham Hong Cong^{1,2}, Dao Huy Bich¹, Nguyen Dinh Duc^{1,*}

¹*Vietnam National University, Hanoi, 144 Xuan Thuy, Cau Giay, Hanoi, Vietnam*

²*Centre for Informatics and Computing, Vietnam Academy of Science and Technology, 18 Hoang Quoc Viet, Cau Giay, Hanoi, Vietnam*

Received 06 October 2014

Revised 22 January 2015; Accepted 10 March 2015

Abstract: This paper deals with an analysis on the supersonic flutter characteristics of Functionally Graded (FGM) plate under aerodynamic loads. Based upon the classical plate theory and the Ilyushin supersonic aerodynamic theory, the governing equations of FGM plates lying in the moving supersonic airflow are derived. The application of Galerkin method with an approximate two-terms Fourier expansion solution leads to a set of nonlinear auto-oscillation equations for determining the nonlinear flutter response and critical velocity. Numerical results are obtained by fourth-order Runge-Kutta method. The influences of the material properties, geometrical parameters and initial conditions on the supersonic flutter characteristics of FGM plate are investigated. The validation of present formulation is carried out.

Keywords: Nonlinear flutter response, critical velocity, functionally graded (FGM) plate, Ilyushin supersonic aerodynamic theory.

1. Introduction

Functionally Graded Materials (FGMs) are composite and microscopically in homogeneous materials with mechanical and thermal properties varying smoothly and continuously from one surface to the other. Typically, these materials are made from a mixture of metal and ceramic or a combination of different metals by gradually varying the volume fraction of the constituents. Due to the high heat resistance, FGMs have many practical applications, such as reactor vessels, aircrafts, space vehicles, defense industries and other engineering structures.

Suppose functionally graded (FGM) structures moving with supersonic velocity V in the airflow or lying in the moving supersonic airflow with velocity V . When the velocity reaches a critical value, in the structures appears the elastic and aerodynamic phenomenon, in which the amplitude increases

* Corresponding author: Tel.: 84- 915966626
Email: ducnd@vnu.edu.vn

continuously, so called flutter. The researches of the flutter play important role in the safety of flight vehicles with high speeds. Therefore flutter phenomena are to be considered and studied by many researchers.

In recent years, many investigations have been carried out on the flutter of FGM plates and shells. Nonlinear thermal flutter of functionally graded panels under a supersonic flow has been investigated by Sohn and Kim [1] using the first-order shear deformation theory. In [1], the first-order piston theory is adopted to represent aerodynamic pressures induced by supersonic airflows. Singha and Mandal [2] studied supersonic flutter characteristics of composite cylindrical panels using a 16-noded isoparametric degenerated shell element. Flutter of flat rectangular anisotropic plate in high mach number supersonic flow have been analyzed by Ramkumar and Weisshaar [3]. Prakash et al. [4] carried out a finite element study on the large amplitude flexural vibration characteristics of FGM plates under aerodynamic load. Ganapathi and Touratier [5] studied supersonic flutter analysis of thermally stressed laminated composite flat panels using the first-order high Mach number approximation to linear potential flow theory. Kouchakzadeh, Rasekh and Haddadpour [6] investigated panel flutter analysis of general laminated composite plates. In [7], Maloy, Shingha and Ganapathi analyzed a parametric study on supersonic flutter behavior of laminated composite skew flat panels. Prakash and Ganapathi [8] examined supersonic flutter characteristics of functionally graded flat panels including thermal effects using the finite element procedure. In [8], the aerodynamic force is evaluated by considering the first order high Mach number approximation to linear potential flow theory. Haddadpour et al. [9] investigated supersonic flutter prediction of functionally graded cylindrical. Recently, Navid Valizadeh et al. [10] studied flutter of FGM plates using NURBS with finite element analysis. Supersonic flutter prediction of functionally graded conical shells was considered by Mahmoudkhani et al. [11]. Shih-Yao Kuo [12] studied flutter of rectangular composite plates with variable fiber pacing applying the finite element method and quasi-steady aerodynamic theory.

Commonly in the considered studies the aerodynamic pressure load was used according to the supersonic piston theory.

The expression of nonlinear aerodynamic load obtained from the Ilyushin supersonic aerodynamic theory [13] was used in the works of Stepanov [14] and Oghibalov [15] for investigating supersonic flutter behavior of isotropic plates lying in the moving supersonic airflow.

The present paper deals with the formulation of a flutter problem of functionally graded plates lying in the moving supersonic airflow or conversely FGM plates moving with supersonic velocity in the airflow. This formulation is based on the classical plate theory and the Ilyushin nonlinear supersonic aerodynamic theory. Investigations on nonlinear flutter response of FGM plates and critical velocity are carried out.

2. Governing equations

Consider a rectangular FGM plate, which is referred to a cartesian coordinate system x, y, z , where (x, y) plane on the midplane of the plate and z on thickness directions, $(-h/2 \leq z \leq h/2)$. The length, width, and total thickness of the plate are a , b and h , respectively. The plate is lying in the

moving supersonic airflow move with velocity V along direction x (Fig. 1), or conversely FGM plate moves with supersonic velocity in the airflow.

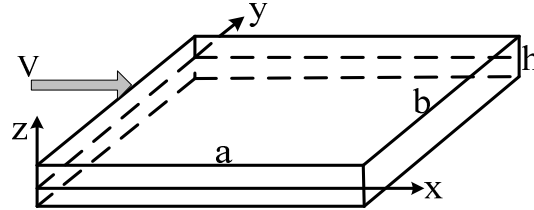


Fig. 1. Geometry of the FGM plate.

By applying a simple power-law distribution (P-FGM), the volume fractions of metal and ceramic, V_m and V_c , are assumed as:

$$V_c(z) = \left(\frac{2z+h}{2h} \right)^N; V_m(z) = 1 - V_c(z), \quad (1)$$

where the volume fraction index N is a nonnegative number that defines the material distribution and can be chosen to optimize the structural response.

The effective properties P_{eff} of the FGMs are determined by the modified mixed rules as follows:

$$P_{eff}(z) = Pr_c V_c(z) + Pr_m V_m(z). \quad (2)$$

In which Pr is a symbol for the specific nature of the material such as elastic modulus E , mass density ρ , and subscripts m and c stand for the metal and ceramic constituents, respectively.

From Eqs. (1) and (2), the effective properties of the FGM plate can be written as follows:

$$[E(z), \rho(z)] = [E_m, \rho_m] + [E_{cm}, \rho_{cm}] \left(\frac{2z+h}{2h} \right)^N, \quad (3)$$

where

$$E_{cm} = E_c - E_m, \rho_{cm} = \rho_c - \rho_m, \quad (4)$$

and the Poisson ratio $\nu(z)$ is assumed to be constant $\nu(z) = \nu$.

2.1. Nonlinear analysis on flutter of FGM plates

In the present study, the classical plate theory is used to obtain the motion and compatibility equations.

The strain-displacement relations taking into account the von Karman nonlinear terms are [16]:

$$\begin{pmatrix} \epsilon_x \\ \epsilon_y \\ \gamma_{xy} \end{pmatrix} = \begin{pmatrix} \epsilon_x^0 \\ \epsilon_y^0 \\ \gamma_{xy}^0 \end{pmatrix} + z \begin{pmatrix} \chi_x \\ \chi_y \\ 2\chi_{xy} \end{pmatrix}, \quad (5)$$

with

$$\begin{aligned}\varepsilon_x^0 &= \frac{\partial u}{\partial x} + \frac{1}{2} \left(\frac{\partial w}{\partial x} \right)^2; \varepsilon_y^0 = \frac{\partial v}{\partial y} + \frac{1}{2} \left(\frac{\partial w}{\partial y} \right)^2; \gamma_{xy}^0 = \frac{\partial u}{\partial y} + \frac{\partial v}{\partial x} + \frac{\partial w}{\partial x} \frac{\partial w}{\partial y}, \\ \chi_x &= -\frac{\partial^2 w}{\partial x^2}; \chi_y = -\frac{\partial^2 w}{\partial y^2}; \chi_{xy} = -\frac{\partial^2 w}{\partial x \partial y},\end{aligned}\quad (6)$$

where ε_x^0 and ε_y^0 are the normal strains, γ_{xy}^0 is the shear strain at the middle surface of the plate, χ_{ij} are the curvatures, and u, v, w are displacement components corresponding to the coordinate directions (x, y, z) .

From Eqs. (6) the geometrical compatibility equation can be written as:

$$\frac{\partial^2 \varepsilon_x^0}{\partial y^2} + \frac{\partial^2 \varepsilon_y^0}{\partial x^2} - \frac{\partial^2 \gamma_{xy}^0}{\partial x \partial y} = \left(\frac{\partial^2 w}{\partial x \partial y} \right)^2 - \frac{\partial^2 w}{\partial x^2} \frac{\partial^2 w}{\partial y^2}.\quad (7)$$

Hooke's law for a plate is defined as follows:

$$\sigma_x = \frac{E}{1-\nu^2} (\varepsilon_x + \nu \varepsilon_y); \sigma_y = \frac{E}{1-\nu^2} (\varepsilon_y + \nu \varepsilon_x); \sigma_{xy} = \frac{E}{2(1+\nu)} \gamma_{xy},\quad (8)$$

The force and moment resultants of the plate can be expressed in terms of stress components across the plate thickness as

$$(N_i, M_i) = \int_{-h/2}^{h/2} \sigma_i(1, z) dz, i = x, y, xy.\quad (9)$$

Inserting Eqs. (3), (5) and (8) into Eq. (9) gives the constitutive relations as

$$\begin{aligned}N_x &= \frac{E_1}{1-\nu^2} (\varepsilon_x^0 + \nu \varepsilon_y^0) + \frac{E_2}{1-\nu^2} (\chi_x + \nu \chi_y), \\ N_y &= \frac{E_1}{1-\nu^2} (\varepsilon_y^0 + \nu \varepsilon_x^0) + \frac{E_2}{1-\nu^2} (\chi_y + \nu \chi_x), \\ N_{xy} &= \frac{E_1}{2(1+\nu)} \gamma_{xy}^0 + \frac{E_2}{1+\nu} \chi_{xy},\end{aligned}\quad (10a)$$

$$\begin{aligned}M_x &= \frac{E_2}{1-\nu^2} (\varepsilon_x^0 + \nu \varepsilon_y^0) + \frac{E_3}{1-\nu^2} (\chi_x + \nu \chi_y), \\ M_y &= \frac{E_2}{1-\nu^2} (\varepsilon_y^0 + \nu \varepsilon_x^0) + \frac{E_3}{1-\nu^2} (\chi_y + \nu \chi_x), \\ M_{xy} &= \frac{E_2}{2(1+\nu)} \gamma_{xy}^0 + \frac{E_3}{1+\nu} \chi_{xy},\end{aligned}\quad (10b)$$

where

$$\begin{aligned}
 E_1 &= E_m h + \frac{E_{cm} h}{N+1}; E_2 = E_{cm} h^2 \left(\frac{1}{N+2} - \frac{1}{2(N+1)} \right), \\
 E_3 &= \frac{E_m h^3}{12} + E_{cm} h^3 \left[\frac{1}{N+3} - \frac{1}{N+2} + \frac{1}{4(N+1)} \right],
 \end{aligned}
 \tag{11}$$

For using later, the reverse relations are obtained from Eq. (10a)

$$\begin{aligned}
 \varepsilon_x^0 &= \frac{1}{E_1} (N_x - \nu N_y - E_2 \chi_x); \varepsilon_y^0 = \frac{1}{E_1} (N_y - \nu N_x - E_2 \chi_y), \\
 \gamma_{xy}^0 &= \frac{2}{E_1} [(1+\nu) N_{xy} - E_2 \chi_{xy}].
 \end{aligned}
 \tag{12}$$

The equations of motion are [16]:

$$\begin{aligned}
 \frac{\partial N_x}{\partial x} + \frac{\partial N_{xy}}{\partial y} &= \rho_1 \frac{\partial^2 u}{\partial t^2}, \\
 \frac{\partial N_{xy}}{\partial x} + \frac{\partial N_y}{\partial y} &= \rho_1 \frac{\partial^2 v}{\partial t^2}, \\
 \frac{\partial^2 M_x}{\partial x^2} + 2 \frac{\partial^2 M_{xy}}{\partial x \partial y} + \frac{\partial^2 M_y}{\partial y^2} + N_x \frac{\partial^2 w}{\partial x^2} + 2 N_{xy} \frac{\partial^2 w}{\partial x \partial y} + N_y \frac{\partial^2 w}{\partial y^2} + q &= \rho_1 \frac{\partial^2 w}{\partial t^2},
 \end{aligned}
 \tag{13}$$

where $\rho_1 = \rho_m h + \rho_{cm} h / (N+1)$.

The external force in this study is an aerodynamic pressure load q that is created by a supersonic airflow. It can be determined by the Ilyushin nonlinear supersonic aerodynamic theory as [13]:

$$-q = B \frac{\partial w}{\partial t} - BV \frac{\partial w}{\partial x} - 2B_1 V \frac{\partial w}{\partial t} \frac{\partial w}{\partial x} + B_1 V^2 \left(\frac{\partial w}{\partial x} \right)^2,
 \tag{14}$$

in which

$$B = \frac{\zeta p_\infty}{V_\infty}; B_1 = \frac{\zeta(\zeta+1)p_\infty}{4V_\infty^2},
 \tag{15}$$

and p_∞, V_∞ the pressure and the sound velocity of the quiet airflow (not excited), V is the airflow velocity on the surface structure, ζ is the Politrop index.

Inserting Eq. (14) into Eq. (13) yields:

$$\frac{\partial N_x}{\partial x} + \frac{\partial N_{xy}}{\partial y} = \rho_1 \frac{\partial^2 u}{\partial t^2},
 \tag{16a}$$

$$\frac{\partial N_{xy}}{\partial x} + \frac{\partial N_y}{\partial y} = \rho_1 \frac{\partial^2 v}{\partial t^2},
 \tag{16b}$$

$$\begin{aligned} & \frac{\partial^2 M_x}{\partial x^2} + 2 \frac{\partial^2 M_{xy}}{\partial x \partial y} + \frac{\partial^2 M_y}{\partial y^2} + N_x \frac{\partial^2 w}{\partial x^2} + 2N_{xy} \frac{\partial^2 w}{\partial x \partial y} + N_y \frac{\partial^2 w}{\partial y^2} \\ & = \rho_1 \frac{\partial^2 w}{\partial t^2} + B \frac{\partial w}{\partial t} - BV \frac{\partial w}{\partial x} - 2B_1 V \frac{\partial w}{\partial t} \frac{\partial w}{\partial x} + B_1 V^2 \left(\frac{\partial w}{\partial x} \right)^2. \end{aligned} \tag{16c}$$

Volmir’s assumption can be used in the dynamical analysis [17]. By taking the inertia $\rho_1 \frac{\partial^2 u}{\partial t^2} \rightarrow 0$ and $\rho_1 \frac{\partial^2 v}{\partial t^2} \rightarrow 0$ into consideration because $u \ll w, v \ll w$. The two equations (16a, 16b) are satisfied by introducing the stress function:

$$N_x = \frac{\partial^2 f}{\partial y^2}; N_{xy} = -\frac{\partial^2 f}{\partial x \partial y}; N_y = \frac{\partial^2 f}{\partial x^2}. \tag{17}$$

Putting Eqs. (6) and (12) into Eq. (10) then substituting the obtained result into Eq. (16c), using relations (17) we obtain

$$\begin{aligned} & \rho_1 \frac{\partial^2 w}{\partial t^2} + B \frac{\partial w}{\partial t} - BV \frac{\partial w}{\partial x} - 2B_1 V \frac{\partial w}{\partial t} \frac{\partial w}{\partial x} + B_1 V^2 \left(\frac{\partial w}{\partial x} \right)^2 + D \Delta \Delta w + 2 \frac{\partial^2 f}{\partial x \partial y} \frac{\partial^2 w}{\partial x \partial y} \\ & - \frac{\partial^2 f}{\partial y^2} \frac{\partial^2 w}{\partial x^2} - \frac{\partial^2 f}{\partial x^2} \frac{\partial^2 w}{\partial y^2} = 0, \end{aligned} \tag{18}$$

where $D = \frac{E_1 E_3 - E_2^2}{E_1 (1 - \nu^2)}$.

Inserting Eqs. (12) and (17) into Eq. (7), we have:

$$\frac{1}{E_1} \left(\frac{\partial^4 f}{\partial x^4} + 2 \frac{\partial^4 f}{\partial x^2 \partial y^2} + \frac{\partial^4 f}{\partial y^4} \right) = \left(\frac{\partial^2 w}{\partial x \partial y} \right)^2 - \frac{\partial^2 w}{\partial x^2} \frac{\partial^2 w}{\partial y^2}. \tag{19}$$

The two equations (18) and (19) are the basic equations for analysis of nonlinear flutter response of the FGM plate.

Four edges of the plate are simply supported and freely movable. The associated boundary conditions are

$$\begin{aligned} & w = N_{xy} = M_x = 0, N_x = 0, \text{ at } x = 0, a, \\ & w = N_{xy} = M_y = 0, N_y = 0, \text{ at } y = 0, b. \end{aligned} \tag{20}$$

The approximate two-terms Fourier expansion solution of the system of Eqs. (18) and (19) satisfying the boundary conditions (20) can be written as

$$w = W_1 \sin \frac{\pi x}{a} \sin \frac{\pi y}{b} + W_2 \sin \frac{2\pi x}{a} \sin \frac{\pi y}{b}, \tag{21}$$

W_1, W_2 - the amplitudes which are functions dependent on time.

Substituting Eq. (21) into the compatibility Eq. (19), and solving the obtained equation, the stress function can be defined as:

$$f = F_1 \cos \frac{2\pi y}{b} + F_2 \cos \frac{2\pi x}{a} + F_3 \cos \frac{4\pi x}{a} + F_4 \cos \frac{\pi x}{a} \cos \frac{2\pi x}{a} + F_5 \cos \frac{2\pi y}{b} \cos \frac{\pi x}{a} \cos \frac{2\pi x}{a} + F_6 \sin \frac{2\pi x}{a} \sin \frac{\pi x}{a} + F_7 \cos \frac{2\pi y}{b} \sin \frac{2\pi x}{a} \sin \frac{\pi x}{a}, \quad (22)$$

in which

$$F_1 = \frac{E_1 b^2}{16a^2} \left(\frac{1}{2} W_1^2 + 2W_2^2 \right); F_2 = \frac{E_1 a^2}{32b^2} W_1^2; F_3 = \frac{E_1 a^2}{128b^2} W_2^2, \\ F_4 = -\frac{2}{9} \frac{E_1 a^2}{b^2} W_1 W_2; F_5 = \frac{2E_1 a^2 b^2 (16a^4 + 80a^2 b^2 + 91b^4)}{81b^8 + 720a^2 b^6 + 1888a^4 b^4 + 1280a^6 b^2 + 256a^8} W_1 W_2, \\ F_6 = -\frac{5}{18} \frac{E_1 a^2}{b^2} W_1 W_2; F_7 = \frac{E_1 a^2 b^2 (328a^2 b^2 + 365b^4 + 80a^4)}{2(81b^8 + 720a^2 b^6 + 1888a^4 b^4 + 1280a^6 b^2 + 256a^8)} W_1 W_2. \quad (23)$$

Replacing Eqs. (21) and (22) into the equations of motion (18) and then applying Galerkin method yields:

$$\frac{\bar{\rho}_1 B_a V_0^2}{4B_h^2} \frac{\partial^2 \bar{W}_1}{\partial \tau^2} + \frac{BV_0}{4B_h} \frac{\partial \bar{W}_1}{\partial \tau} + \frac{4B_a B_1 V V_0}{3B_h^2} \frac{\partial \bar{W}_1}{\partial \tau} \bar{W}_2 - \frac{2B_a B_1 V V_0}{3B_h^2} \frac{\partial \bar{W}_2}{\partial \tau} \bar{W}_1 \\ + l_{11} \bar{W}_1 + l_{12} \bar{W}_2 + l_{13} \bar{W}_1^2 + l_{14} \bar{W}_2^2 + l_{15} \bar{W}_1^3 + l_{16} \bar{W}_1 \bar{W}_2^2 = 0, \quad (24a)$$

$$\frac{\bar{\rho}_1 B_a V_0^2}{4B_h^2} \frac{\partial^2 \bar{W}_2}{\partial \tau^2} - \frac{2B_a B_1 V V_0}{3B_h^2} \frac{\partial \bar{W}_1}{\partial \tau} \bar{W}_1 + \frac{BV_0}{4B_h} \frac{\partial \bar{W}_2}{\partial \tau} + l_{21} \bar{W}_1 \\ + l_{22} \bar{W}_2 + l_{23} \bar{W}_1 \bar{W}_2 + l_{24} \bar{W}_2^3 + l_{25} \bar{W}_1^2 \bar{W}_2 = 0, \quad (24b)$$

in which

$$l_{11} = \frac{\bar{D}\pi^4}{4B_h^4 B_a} (B_a^2 + 1)^2; l_{12} = \frac{2BV}{3B_h}, \\ l_{13} = \frac{8B_a B_1 V^2}{9B_h^2}; l_{14} = \frac{224B_a B_1 V^2}{45B_h^2}; l_{15} = \frac{\bar{E}_1 \pi^4}{64B_h^2} \left(\frac{B_a^3}{B_h^2} + \frac{1}{B_a B_h^2} \right), \\ l_{16} = \frac{\frac{\bar{E}_1 \pi^4}{B_a B_h^4} \left(\frac{16}{B_a^4} + \frac{80}{B_a^2} + 91 \right)}{2 \left(81 + \frac{720}{B_a^2} + \frac{1888}{B_a^4} + \frac{1280}{B_a^6} + \frac{256}{B_a^8} \right)} \\ + \frac{\frac{5\bar{E}_1 \pi^4}{B_a B_h^4} \left(\frac{328}{B_a^2} + 365 + \frac{80}{B_a^4} \right)}{32 \left(81 + \frac{720}{B_a^2} + \frac{1888}{B_a^4} + \frac{1280}{B_a^6} + \frac{256}{B_a^8} \right)} + \frac{\bar{E}_1 \pi^4}{16B_a B_h^4} + \frac{\bar{E}_1 B_a^3 \pi^4}{16B_h^4}, \quad (25)$$

$$\begin{aligned}
 l_{21} &= -\frac{2BV}{3B_h}; l_{22} = \frac{\pi^4 \bar{D}}{4B_a B_h^4} (4B_a^2 + 1)^2, \\
 l_{23} &= \frac{64B_a B_1 V^2}{45B_h^2}; l_{24} = \frac{\bar{E}_1 B_a^3 \pi^4}{4B_h^4} + \frac{\bar{E}_1 \pi^4}{64B_a B_h^4}, \\
 l_{25} &= \frac{\frac{\bar{E}_1 \pi^4}{B_a B_h^4} \left(\frac{16}{B_a^4} + \frac{80}{B_a^2} + 91 \right)}{2 \left(81 + \frac{720}{B_a^2} + \frac{1888}{B_a^4} + \frac{1280}{B_a^6} + \frac{256}{B_a^8} \right)} \\
 &+ \frac{\frac{5\pi^4 \bar{E}_1}{B_a B_h^4} \left(\frac{328}{B_a^2} + 365 + \frac{80}{B_a^4} \right)}{32 \left(81 + \frac{720}{B_a^2} + \frac{1888}{B_a^4} + \frac{1280}{B_a^6} + \frac{256}{B_a^8} \right)} + \frac{\bar{E}_1 \pi^4}{16B_a B_h^4} + \frac{\bar{E}_1 B_a^3 \pi^4}{16B_h^4}, \\
 \bar{W}_1 &= \frac{W_1}{h}; \bar{W}_2 = \frac{W_2}{h}; \tau = \frac{V_0 t}{a}; B_a = b/a; B_h = b/h; \bar{D} = D/h^3; \bar{E}_1 = E_1/h; \\
 \bar{\rho}_1 &= \rho_1/h.
 \end{aligned} \tag{25}$$

The system of motion equations (24) will be used to determine the nonlinear flutter response of FGM plates.

3. Numerical results and discussion

The problem is treated as that of finding out solutions of Eqs. (24a) and (24b) (the dynamic responses) for different values of the airflow velocity and determining the value of velocity when appears the phenomenon such as the vibration amplitude is found to increase continuously during the consideration period. This value of velocity is called a critical flutter velocity and the instability of FGM plate happens.

3.1. Validation of the present formulation

To check the reliability of the approach in this paper, the parameters of the isotropic plate in [14, 15] are used:

$$\begin{aligned}
 E &= 2.10^6 \text{ kg / cm}^2, \rho_0 = 7.8.10^{-3} \text{ kg / cm}^3 \\
 \text{and } \zeta &= 1.4, p_\infty = 1.014 \frac{\text{kG}}{\text{cm}^2}, V_0 = V_\infty = 3.4 \times 10^4 \text{ cm / s}, \\
 \bar{W}_1(0) &= 0.1, \bar{W}_2(0) = 0, \frac{\partial \bar{W}_1(0)}{\partial \tau} = 0, \frac{\partial \bar{W}_2(0)}{\partial \tau} = 0.
 \end{aligned} \tag{26}$$

The nonlinear flutter response of homogeneous isotropic plate is shown in Figure 2 with the velocity $V=1000\text{ m/s}$. In this case, the plate has unstable state. Comparing with the result recognized in the work [15] (Fig.17 of [15]), it can see that the good agreements are observed (figure 3).

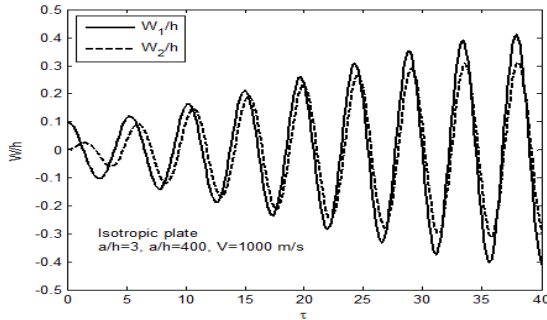


Fig. 2. Nonlinear flutter response for isotropic plate in the present approach.

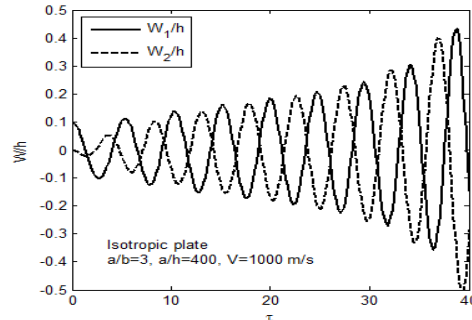


Fig. 3. Nonlinear flutter response for isotropic plate of Ilyushin [15].

3.2. Nonlinear flutter response. Critical supersonic velocity

The fourth-order Runge–Kutta method is used to solve Eqs. (24). In order to illustrate the present approach, we consider a ceramic-metal FGM plate that consists of aluminum (metal) and alumina (ceramic) with the material characteristics [8]:

$$\begin{aligned} E_c &= 380 \times 10^9 \text{ N/m}^2, \rho_c = 3800 \text{ kg/m}^3, \\ E_m &= 70 \times 10^9 \text{ N/m}^2, \rho_m = 2702 \text{ kg/m}^3, \\ \nu &= 0.3, \end{aligned} \quad (27)$$

and the characteristics of supersonic airflow [15] as following:

$$\zeta = 1.4, p_\infty = 1.014 \frac{\text{kG}}{\text{cm}^2}, V_0 = V_\infty = 3.4 \times 10^4 \text{ cm/s.}$$

with initial conditions of the plate:

$$\begin{aligned} \bar{W}_1(0) &= 0.01; \bar{W}_2(0) = 0, \\ \frac{\partial \bar{W}_1(0)}{\partial \tau} &= 0; \frac{\partial \bar{W}_2(0)}{\partial \tau} = 0. \end{aligned} \quad (28)$$

The nonlinear dynamic responses of the geometric parameters $a/b=3, a/h=400$ and volume fraction index $N=1$ are shown in figures 4, 5 and 6. Fig. 4 and Fig. 6 show that when increasing velocity ($800 \div 900 \text{ m/s}$) the nonlinear dynamic response with amplitudes W_1/h and W_2/h of the plate is observed to change from steady-flute to unstable. When $V < 854.83 \text{ m/s}$ the oscillation of FGM plate is damped (steady state), $V = 854.83 \text{ m/s}$ the FGM plate fluctuates almost as conditioning (critical status). When $V > 854.83 \text{ m/s}$ the oscillations of FGM plate increase continuously with time (unstable state), it may lead to destruction of FGM plate.

Thus, the flutter critical velocity of FGM plate can be taken as $V_{\text{Critical}} = 854.83 \text{ m/s}$.

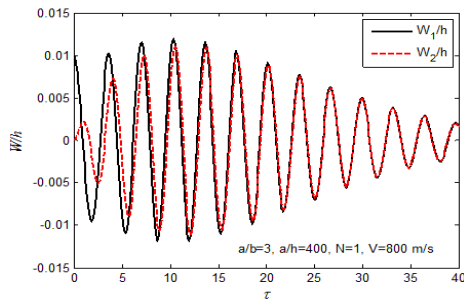


Fig. 4. Nonlinear flutter response of FGM plate at $V = 800 \text{ m/s}$.

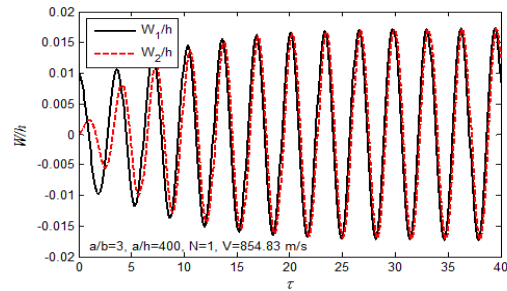


Fig. 5. Nonlinear flutter response of FGM plate at $V = 854.83 \text{ m/s}$.

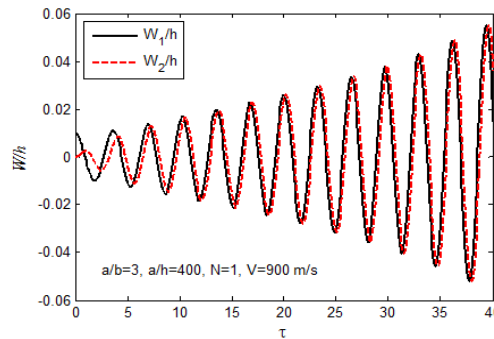


Fig. 6. Nonlinear flutter response of FGM plate at $V = 900 \text{ m/s}$.

Fig. 7 shows the phase diagram $\frac{\partial(W_1/h)}{\partial\tau}$ and $\frac{W_1}{h}$ in the case of instability (Fig. 6), the nature of the instability phenomenon is evident in this phase diagram. It is observed that the phase diagram is found as a spiral schema derived from the IC (Initial Cycle) at $(t=0)$ (Fig.7), the IC is the top of spiral, then it expands with increasing amplitude (divergence phenomenon). This phase diagram of the plate corresponds to an unstable state.

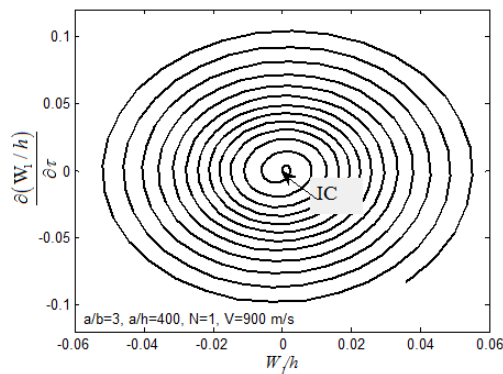


Fig. 7. Phase diagram at $V = 900 \text{ m/s}$.

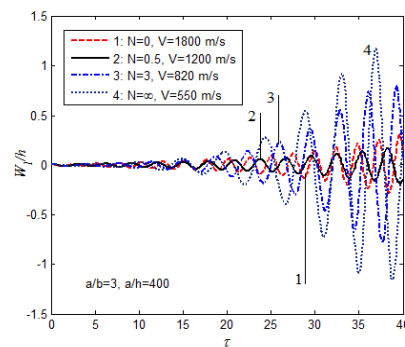


Fig. 8. Effect of volume fraction index on nonlinear flutter response of FGM plate.

Effect of volume fraction index N on nonlinear flutter response of the FGM plate is shown in Fig. 8 and Tab. 1. As can see that increasing the volume fraction index N leads to reduce the critical flutter velocity. This is clear because the elastic modulus of metal is much lower than that of ceramic.

Table 1. Effect of the volume fraction index (N) and geometrical parameters on critical flutter velocity.

	$a/b=3$			$a/h=400$		
	$a/h=300$	$a/h=400$	$a/h=500$	$a/b=2$	$a/b=3$	$a/b=4$
$N=0$	4000	1800	900	960	1800	2750
$N=0.5$	2700	1200	700	780	1200	1800
$N=1$	2060	855	650	600	855	1500
$N=2$	1600	835	580	550	835	1100
$N=3$	1450	820	530	500	820	1000
$N=5$	1390	760	500	390	760	950
$N=7$	1290	650	480	350	650	920
$N=\infty$	970	550	390	290	550	830

Figures 9, 10 and table 1 show effect of geometrical parameters on nonlinear flutter response of FGM plate and critical flutter velocity ($V_{critical}$).

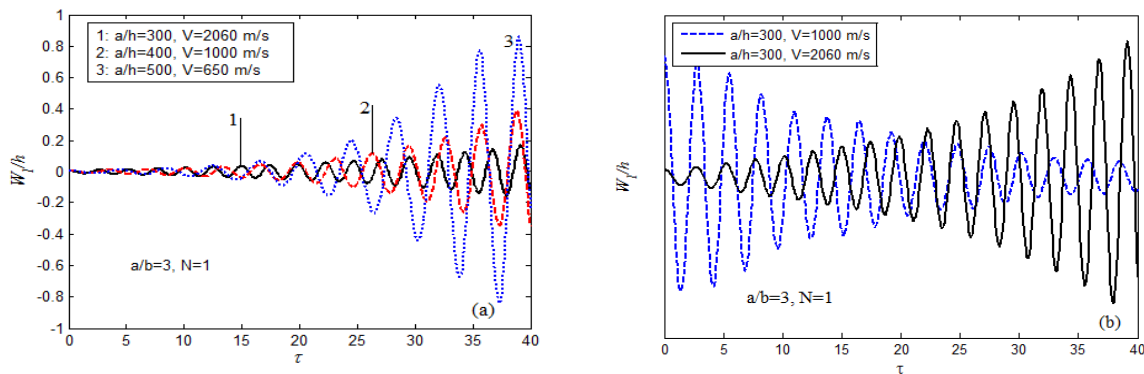


Fig. 9. Effect of a/h ratio on nonlinear flutter response of FGM plate.

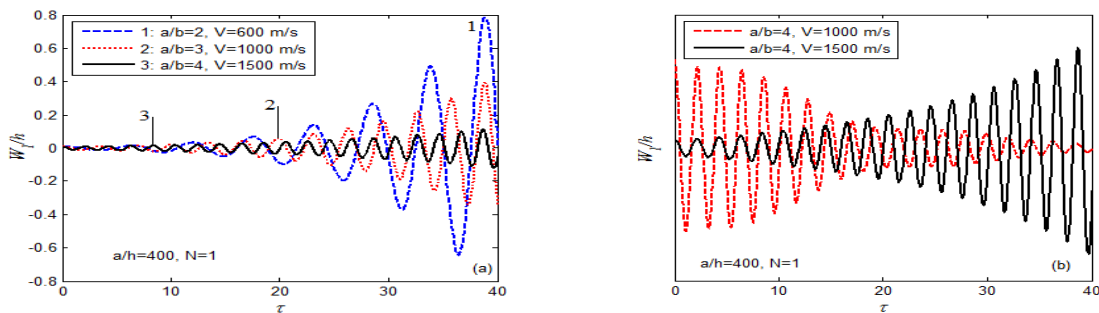


Fig. 10. Effect of a/b ratio on nonlinear flutter response of FGM plate.

From the figure 9(a) finding that the ratio $a/h=300, a/h=400, a/h=500$ respectively the velocity $V=2060\text{ m/s}, V=1000\text{ m/s}, V=650\text{ m/s}$, the plate in the instable state (here is the critical velocity). In the case of $a/h=300$ with $V=1000\text{ m/s}$ the plate is still in the steady state, increasing $V=2060\text{ m/s}$ the plate turns into the instable state - figure 9(b). That shows the influence of ratio a/h on nonlinear flutter of FGM plate. Increasing the ratio a/h will reduce the value of the flutter critical velocity (V_{critical}), or make the plate more easily destroyed.

The influence of the ratio a/b on the nonlinear flutter of the plate is shown in figure 10. Figure 10(a) indicates that with the ratio $a/b=2, a/b=3, a/b=4$ respectively the velocities $V=600\text{ m/s}, V=1000\text{ m/s}, V=1500\text{ m/s}$, the plate is in the instable state (corresponding to the critical velocity). In the case of $a/b=4, V=1000\text{ m/s}$ the plate is still in the steady state, increasing $V=1500\text{ m/s}$ the plate turns into the instable state (Fig.10(b)). That shows the influence of the ratio a/b on the nonlinear flutter of the FGM plate. Consequently, increasing the ratio a/b , the value of the critical velocity flutter (V_{critical}) will increase.

The influence of initial conditions on the nonlinear flutter is shown in figure 11. The results show that the different initial conditions lead to meet the nonlinear dynamic flutter and the different critical velocities.

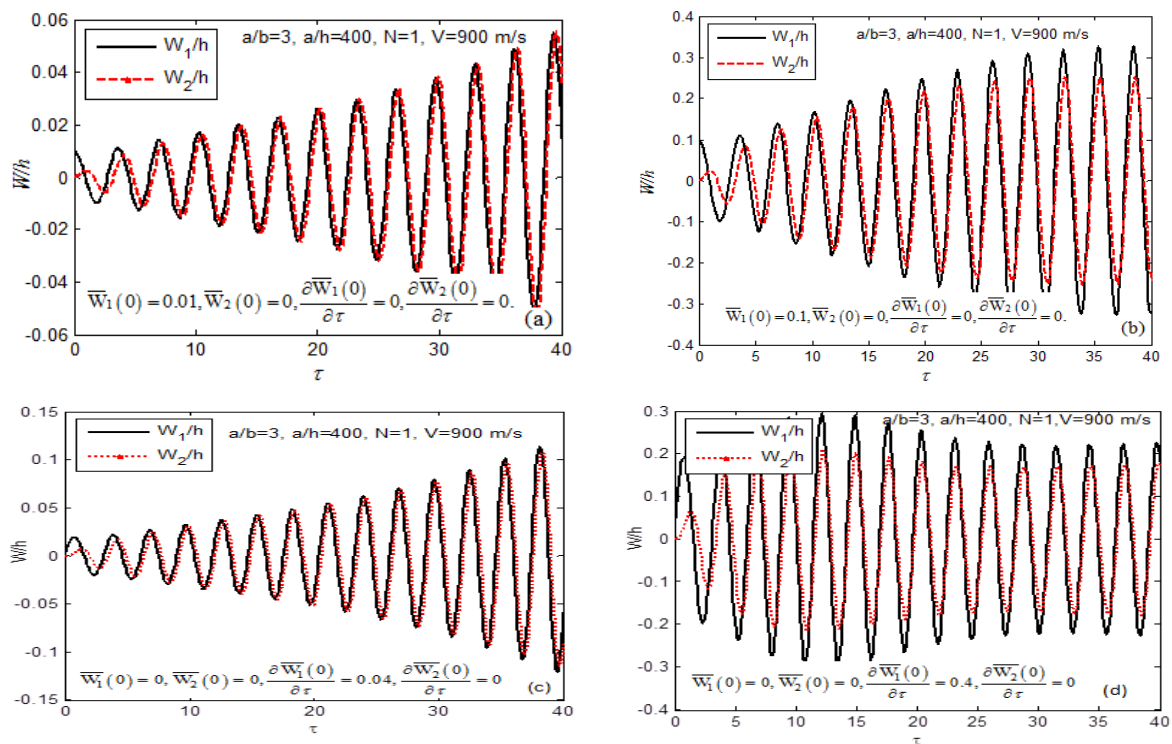


Fig. 11. Effect of initial conditions on nonlinear flutter response of FGM plate.

The results in figure 11(a) and 11(b) present the effect of initial deflection $\overline{W}_1(0)$ on nonlinear flutter of the plate: amplitudes are increased with increasing initial deflections.

Figure 11(c) is drawn with the value of the initial condition $\overline{W}_1(0) = 0, \overline{W}_2(0) = 0, \frac{\partial \overline{W}_1(0)}{\partial \tau} = 0.04, \frac{\partial \overline{W}_2(0)}{\partial \tau} = 0$ the plate is in the instable state while figure 11(d) is drawn to the initial condition $\overline{W}_1(0) = 0, \overline{W}_2(0) = 0, \frac{\partial \overline{W}_1(0)}{\partial \tau} = 0.4, \frac{\partial \overline{W}_2(0)}{\partial \tau} = 0$ the plate is still in the steady state. The figures 11(c) and 11(d) show significantly the effects of initial velocity on nonlinear flutter of the plate. Therefore, the velocity is one of the important factors which can be used to actively control the flutter of the FGM plates

4. Conclusions

The paper obtained some main results as the following

(i) The nonlinear governing equations for flutter analysis of FGM plates lying in the moving supersonic airflow based on the classical plate theory and the Ilyushin nonlinear aerodynamic theory are derived.

(ii) Using the stress function, the Galerkin method and an approximate two-terms Fourier expansion solution, the nonlinear differential auto-oscillation equations are solved for analysing supersonic flutter characteristics of FGM plates.

(iii) From numerical results, we can conclude that:

- The volume fraction index N increases, i.e. the ceramic material constituent decreases, then the critical velocity of the supersonic airflow decreases, the FGM plate is more easily instable.

- The geometrical parameters importantly impact on the flutter of the FGM plates. Ratio a/b increases, the critical velocity of flutter increases and ratio a/h increases, the critical velocity of flutter decreases.

- Initial conditions significantly effect on the nonlinear flutter response and the critical velocity of the FGM plate.

Acknowledgements

This paper was supported by Grant in Mechanics “*Nonlinear analysis on stability and dynamics of functionally graded shells with special shapes*”- code QG.14.02 of Vietnam National University, Hanoi. The authors are grateful for this support.

References

- [1] L.J. Sohn, J.H. Kim, Nonlinear thermal flutter of functionally graded panels under a supersonic flow, J. Composite Structures, 88, 380-387, 2009.

- [2] M.K. Singha, Mukul Mandal, Supersonic flutter characteristics of composite cylindrical panels, *J. Composite Structure*, 82, 295-301, 2008.
- [3] R.L. Ramkumar, T.A. Weisshaar, Flutter of flat rectangular anisotropic plate in high mach number supersonic flow, *J. of Sound and Vibration*, 50(4), 587-597, 1977.
- [4] T. Prakash, M.K. Singha, M. Ganapathi, A finite element study on the large amplitude flexural vibration characteristics of FGM plates under aerodynamic load, *International Journal of Non-Linear Mechanics*, 47, 439-447, 2012.
- [5] M. Ganapathi, M. Touratier, Supersonic flutter analysis of thermally stressed laminated composite flat panels, *J. Composite Structures*, 34, 241-248, 1996.
- [6] M.A. Kouchakzadeh, M. Rasekh, H. Haddadpour, Panel flutter analysis of general laminated composite plates, *J. Composite Structure*, 92, 2906-2915, 2010.
- [7] Maloy K. Shingha, M. Ganapathi, A parametric study on supersonic flutter behavior of laminated composite skew flat panels, *J. Composite Structures*, 69, 55-63, 2005.
- [8] T. Prakash, M. Ganapathi, Supersonic flutter characteristics of functionally graded flat panels including thermal effects, *J. Composite Structures*, 72, 10-18, 2016.
- [9] H. Haddadpour, S. Mahmoudkhani, H.M. Navazi, Supersonic flutter prediction of functionally graded cylindrical, *J. Composite Structures*, 83, 391-398, 2008.
- [10] Navid Valizadeh, Sundararajan Natarajan, Octavio A. Gonzalez-Estrada, Timon Rabczuk, Tinh Quoc Bui, Stephane P.A. Bordas, NURBS-based finite element analysis of functionally graded plates: Static bending, vibration, buckling and flutter, *J. Composite Structures*, 99, 309-326, 2013.
- [11] S. Mahmoudkhani, H. Haddadpour, H.M. Navazi, Supersonic flutter prediction of functionally graded conical shells, *J. Composite Structure*, 92, 377-386, 2010.
- [12] Shih-Yao Kuo, Flutter of rectangular composite plates with variable fiber pacing, *J. Composite Structure*, 93, 2533-2540, 2011.
- [13] A.A. Ilyushin, The law of plane cross sections in supersonicaerodynamics, *J. of Applied Mathematics and Mechanics*, 20 (6) (1956), (in Russian) .
- [14] R.D. Stepanov. On the flutter problem of plates. *Machinery and equipment*. 2 (1960), (in Russian).
- [15] P.M. Oghibalov, Problems of dynamics and stability of shells. Moscow University Press (1963), 164-174, (in Russian).
- [16] J.N. Reddy, *Mechanics of laminated composite plates and shells: theory and analysis*. Boca Raton: CRC Press, (2004).
- [17] S. Volmir, *Nonlinear dynamic of plates and shells*, Science edition, (1972).